1974

Rigid Body Vibrations of Compressors

C. H. Gerhold
Purdue University

J. F. Hamilton
Purdue University

RIGID BODY VIBRATIONS OF COMPRESSORS

Carl H. Gerhold
Graduate Research Assistant

James F. Hamilton
Professor of Mechanical Engineering

Ray W. Herrick Laboratories
School of Mechanical Engineering
Purdue University
West Lafayette, Indiana 47907

INTRODUCTION

The following paper presents the development of a mathematical model for a single cylinder refrigeration compressor. The model is intended to predict the displacements of the compressor's suspension mounting points and its frame center of gravity during both steady-state and transient shutdown operation. Preliminary comparison is made with previously obtained experimental data for this compressor in terms of magnitudes of deflection of the C.G. and mounting points. While it was found that discrepancies existed between the model predictions and the experimental results, it is felt that the model was in sufficiently good agreement with experiment and that the disagreement was due to measurements in the system parameters. A discussion of the extension of the model to compressors of different types is given.

The model is developed from a summation of the energy expressions written for each of the major components of the compressor, and transformed into a set of second order differential equations by means of Lagrangian techniques. The resulting set of equations is non-linear and are solved numerically.

MODEL DEVELOPMENT

Consider a general rigid body whose motion is constrained in a describable manner within a frame; which in turn, moves in an inertial system, as shown in Figure 1. The rigid body is any compressor element (e.g. piston, crank shaft, etc.) while the frame is the frame casting of the compressor and the inertial reference is the compressor shell.

Translational and Rotational Velocity Terms

Figure 2 shows the vector positions and velocities of the frame and a general compressor element. The translational velocity of the compressor element center of gravity, relative to the inertial frame, is made up of the following components.

$$\vec{V}_{i/I} = \vec{V}_{F/I} + \dot{\vec{r}}_i + (\vec{\omega}_{F/I} \times \vec{r}_i)$$

where:

$\vec{V}_{F/I}$ = the translational velocity vector of the frame C.G. relative to the inertial reference.

$\vec{r}_i$ = the position vector of the compressor element C. G. measured relative to the frame C.G.

$\dot{\vec{r}}_i$ = the time derivative of $\vec{r}$

$\vec{\omega}_{F/I}$ = the angular velocity vector of the frame relative to the inertial reference.

The sum $\dot{\vec{r}}_i + (\vec{\omega}_{F/I} \times \vec{r}_i)$ is denoted $\vec{V}_{i/F}$ in Figure 2.

In the same manner, the angular velocity vector of the compressor element is the sum of the angular velocity of the element relative to the frame and the angular velocity of the frame relative to the inertial reference. From Figure 2:

$$\vec{\omega}_{i/I} = \vec{\Omega}_i + \vec{\omega}_{F/I}$$

where:

$\vec{\Omega}_i$ = the angular velocity vector of the element relative to the frame.

$\vec{\omega}_{F/I}$ = the angular velocity vector defined previously.

Kinetic Energy Expression

With the translational and rotational velocities determined, the total kinetic energy of any compressor element may be written as:

$$T_i = 1/2\ M_i(\vec{V}_{i/I} \cdot \vec{V}_{i/I}) + 1/2 \vec{\omega}_{i/I} \cdot \vec{I} \cdot \vec{\omega}_{i/I}$$

where:

M_i = the mass of the compressor element

$\vec{I}$ = the inertial tensor composed of moments and products of inertia of the compressor element.

with $\vec{V}_{i/I}$ and $\vec{\omega}_{i/I}$ as defined previously.

POTENTIAL AND DISSIPATION ENERGY EXPRESSIONS

For this analysis, it is assumed that the elements undergo motion of a sufficiently small magnitude to consider the potential energy terms arising from their movement in the gravitational field to be negligible. However, potential energy stored and released in the deflection of the suspension springs by which the frame casting is attached to the compressor shell is not small; nor is the energy dissipation due to damping in these springs.

The location at which the spring is affixed to the frame is defined by the position vectors $\vec{ML}_1$, $\vec{ML}_2$, $\vec{ML}_3$, as shown in Figure 3. The motion of any spring mounting point is thus obtainable in terms of the position vectors and of the motions of the frame within the inertial axes. The potential energy expression for any spring is:

$$V = 1/2\vec{\Delta} \cdot \vec{k} \cdot \vec{\Delta}$$

where:

$\vec{\Delta}$ = the vector motion of the spring mounting point from the equilibrium position.

$\vec{k}$ = the spring stiffness vector.

For each spring shown in Figure 3, there is an assumed viscous damping mechanism. The velocity of any spring mounting point is the time derivative of the spring deflection. With these velocities, the dissipation energy expression, for a suspension spring is written:

$$D = 1/2\dot{\vec{\Delta}} \cdot \vec{c} \cdot \dot{\vec{\Delta}}$$

where:

$\vec{c}$ = the viscous damping vector

$\dot{\vec{\Delta}}$ = the time derivative of the spring mounting point motion.

Energy is also dissipated from the system by friction in the bearings on the shaft and in the piston rings.

INPUT FORCING TERMS

The compressor is driven by a torque input on the crankshaft with all reactive forces through the oil film bearing surfaces between the compressor elements assumed to be instantaneous, equal and opposite to the applied forces.

The crank angular displacement, θc, is written as an independent variable in the problem in the following manner. The compressor frame is held fixed, such that there is no translation or rotation of the frame; and all motion is that of the elements within the compressor frame. All motive parts internal to the compressor are connected to, and thus, impelled by, the crankshaft, which rotates as θc. The instantaneous position and velocity terms are then, describable functions of the crank angular displacement. The simplification involves the assumption that the motions of the compressor elements within the frame are the same as those relative to the frame.

Motor Torque

The motor torque is taken from a typical torque-speed curve for a single phase shunt-wound motor, as shown in Figure 4. It is assumed that the variation of crank speed in a cycle is slow enough that the steady state torque-speed curve may be used, and, thus, for a given speed of the compressor during quasi-steady-state operation; a value for the motor torque is known.

Gas Pressure Torque

The gas pressure torque is evaluated according to the P-V diagram shown in Figure 5, for a typical thermodynamic cycle involving a perfect gas (air). During compression or expansion, the gas follows a polytropic line defined by the relationship $PV^n = C$, where the C's are determined from the values of pressure and volume in the cylinder at Bottom Dead Center and Top Dead Center, respectively. With the pressure known as a function of volume, and hence, crank angle, the gas pressure torque is evaluated from the expression relating pressure and torque for a Scotch-Yoke Mechanism.

SYSTEM EQUATIONS OF MOTION

The expressions for the total kinetic, potential and dissipation energies of the compressor may now be converted by use of the Lagrange Equations to yield the following set of differential equations for the compressor

$$\begin{bmatrix} M_{(6\times6)} & 0 \\ 0 & I_{eq} \end{bmatrix} \begin{Bmatrix} \ddot{X} \\ \ddot{\theta}_c \end{Bmatrix} + \begin{bmatrix} C_{(6\times6)} & 0 \\ 0 & C_{eq} \end{bmatrix} \begin{Bmatrix} \dot{X} \\ \dot{\theta}_c \end{Bmatrix} +$$

$$\begin{bmatrix} & \vdots & \\ K_{(6x6)} & \cdots & 0 \\ & \vdots & \\ \cdots & \cdots & \cdots \\ 0 & \cdots & K_{eq} \end{bmatrix} \begin{Bmatrix} X \\ \cdots \\ \theta_c \end{Bmatrix} = \begin{Bmatrix} -Q \\ \cdots \\ Q \end{Bmatrix}$$

The above matrices are 7x7 with the differential equation for θ_c uncoupled as was mentioned previously. C_{eq} in this equation includes a viscous damping term applied to the crankshaft, whose value is estimated by comparing predicted to experimental shutdown times. The generalized coordinate vector {x}, is the frame C.G. translation and the frame rotation. The 6x6 mass matrix [M], includes the masses, products and moments of inertial and the gyroscopic terms. The damping matrix, [C], contains all terms from the differentiated kinetic energy expression which multiply velocities, as well as terms arising from operation on the dissipation energy expression. The stiffness matrix, [K], contains terms from the potential energy expression as well as displacement proportional terms from the kinetic energy expression. Q is the sum of the gas pressure and motor torques used as input to the differential equation for θ_c. It enters, equally and oppositely, into the input vector for the differential equation in {x}. The above matrices also contain terms arising from nonlinear coupling among the generalized coordinates.

The nonlinear, coupled differential equations were solved numerically on a digital computer system using a Runge-Kutta integration technique.

RESULTS

The model was tested in two running modes: 1) Steady-State and 2) Transient Shutdown. It is assumed that at onset of shutdown, the motor torque goes to zero instantly.

STEADY-STATE OPERATION

Crankshaft Motion

Figure 6 shows the crank velocity versus time history predicted by numerical solution of the differential equation in θ_c. The time axis is normalized by the time for one cycle of the compressor. It is seen that during steady-state operation of the compressor, the crank speed is not constant.

Compressor Frame Motion

Insufficient experimental data exists to carry out a definitive comparison of the model's prediction to experimental results of the compressor motion. However, in order to ascertain the model's ability to predict displacements which are in the proper order of magnitude, Table 1 was compiled. The experimental data is taken from information obtained by R.H. Harrison (2); and comparison is made on the magnitudes of displacements of the frame C.G. and the three spring mountings points in the inertial coordinate directions. On the whole, the model's ability to predict orders of magnitudes and relationships of the magnitudes in the various coordinate directions is relatively good.

TRANSIENT SHUTDOWN OPERATION

Crankshaft Motion

From investigations by G.T. Kinney (3) there are three distinct modes of shutdown for the crank. From the model results, these modes correspond most closely to shutdown initiated at: 1) Top Dead Center, 2) Bottom Dead Center, and 3) approximately 150°. It was from these results that the equivalent damping term used the differential equation for θ_c was obtained. When shut-down is initiated at a crank angle of approximately 150°, the crankshaft will stop ultimately at T.D.C. This can be explained by reference to Figure 5. It is seen that the pressure in the cylinder drops off quite rapidly beyond T.D.C. Thus, if the crankshaft exerts sufficient torque to impel the piston to T.D.C.; but the friction in the system, combined with the rapidly equalizing pressure on either side of the piston, are sufficient to overcome the rotatory inertia; crank motion ceases near Top Dead Center position.

Compressor Frame Motion

The crankshaft rotational velocity, and hence, the driving frequency, reduces to the range of the eigenvalues for the system of elements comprising this compressor, in approximately 0.055 seconds after shutdown begins; and the model predicts that this is the point at which the system goes into resonance in the range of frequencies:

$$7.6 \leq f_n \leq 8.13 \quad (Hz)$$

Superimposed on this vibration are the natural frequencies in each coordinate direction of each of the springs on which the compressor is mounted. Resonance for the system composed of the compressor and the mounting springs is in the neighborhood

of 3.97 Hz, and the driving frequency approaches this area within 0.135 seconds after shutdown.

Table 2 is similar to Table 1 in that comparison of the magnitudes of displacement is made in several coordinate directions for the spring mounting points. The experimental results are from data collected by Kinney (3). While it does not predict exactly the magnitudes of deflections; the model does show which of the coordinate directions will predominate and gives an estimate of their respective magnitudes. In considering the differences between the two sets of values in Table 2, this fact should be borne in mind. No accurate indication of the crank position at shutdown is given in the experimental data, and comparison to the experimental values is made for the model shutdown at T.D.C. because the oscilloscope traces of the crankshaft angular displacement versus time history coincide most closely to the predicted history for shutdown at this point. The magnitudes of the various spring mounting points vary by as much as 0.250 inches, depending on whether shutdown occurs at T.D.C. or B.D.C.; but the form of the time histories of the coordinate directions is the same, as are the relative magnitudes among the coordinate directions for any spring mounting point.

CONCLUSIONS

1. The model developed in this paper is capable of predicting trends of vibrational response of the frame center of gravity and of the spring mounting points for a refrigeration compressor.
2. The model is general enough that it can be extended to include compressors of a more complex nature, provided the motions of the major inertial elements within the compressor are describable.
3. The ability to incorporate different suspension systems than that considered here is part of the model.
4. The discrepancies that exist between the predicted and the experimental magnitudes are felt to arise in part from errors in measurement of the system parameters or in the measurement of the compressor motion in the experimental work.

BIBLIOGRAPHY

1. Wells, D.A., Lagrangian Dynamics, Schaum's Outline Series, McGraw-Hill, 1967.
2. Harrison, R.H., Jr., Mathematical and Experimental Analysis of the Vibration of a Refrigeration Compressor, Masters Degree Thesis, Purdue University, 1970.
3. Kinney, G.T., Mathematical Simulation of the Vibration of a Refrigeration Compressor, Masters Degree Thesis, Purdue University, 1968.
4. Gerhold, C.H., Mathematical Model of a Single-Cylinder Compressor, Masters Degree Thesis, Purdue University, 1972.

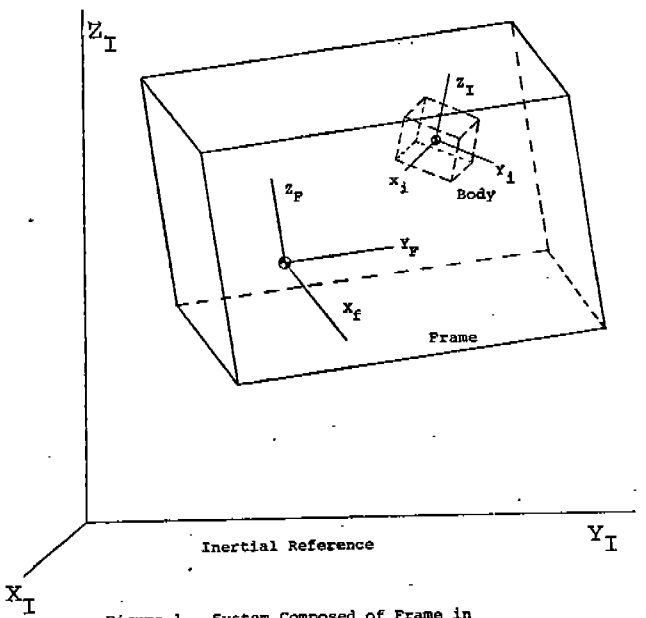

Figure 1. System Composed of Frame in Inertial Reference and Rigid Body Within Frame

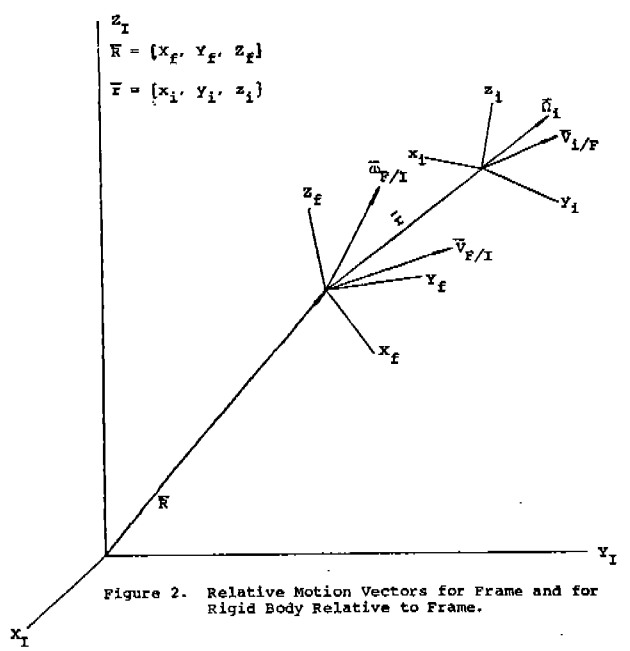

Figure 2. Relative Motion Vectors for Frame and for Rigid Body Relative to Frame.

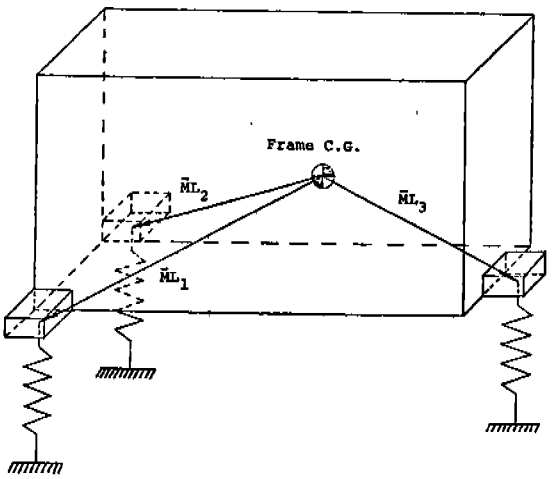

Figure 3. Representation of Positions of Spring Mounting Points and Definition of Mounting Point Locations.

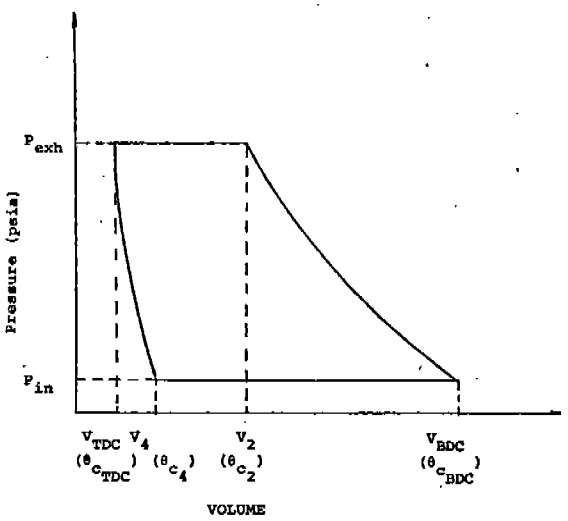

Figure 5. Typical Pressure vs. Volume Curve for Reversible, Polytropic Cycle of an Ideal Gas.

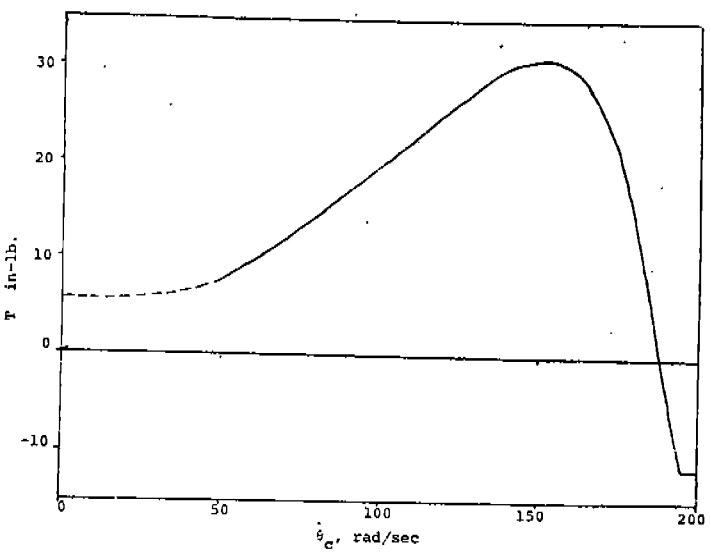

Figure 4. Typical Torque-Speed Curve for 1/4 HP. Shunt-Wound, Single Phase Motor.

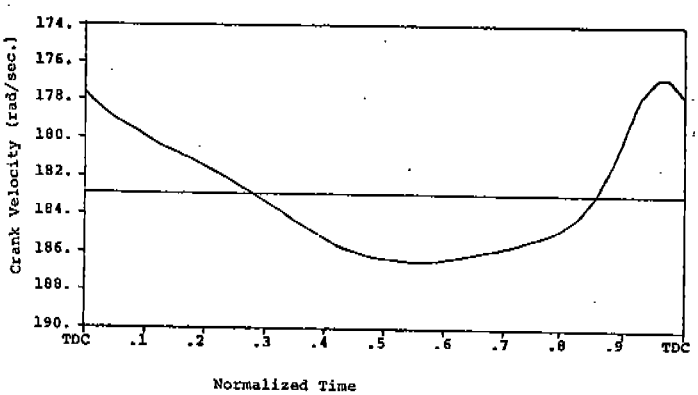

Figure 6. Predicted Steady-State Crank Velocity.

TABLE 1

MAGNITUDE COMPARISON OF PREDICTED AND EXPERIMENTAL MAXIMUM DISPLACEMENTS FOR COMPRESSOR IN STEADY-STATE

Frame C.G.		
Coordinate Direction	Predicted [in(cm)]	Experimental [in(cm)]
X	0.0096 (0.0234)	0.0086 (0.0218)
Y	0.0061 (0.0155)	0.0062 (0.0157)
Z	0.0008 (0.0020)	0.0021 (0.0534)
Spring Mounting Point 1		
Coordinate Direction	Predicted	Experimental
X_1	0.0108 (0.0274)	0.0109 (0.0277)
Y_1	0.0061 (0.0151)	0.0086 (0.0218)
Z_1	0.0079 (0.0201)	0.0085 (0.0216)
Spring Mounting Point 2		
Coordinate Direction	Predicted	Experimental
X_2	0.0059 (0.0150)	0.0082 (0.0208)
Y_2	0.0037 (0.0094)	0.0009 (0.0023)
Z_2	0.0126 (0.0320)	0.0228 (0.0580)
Spring Mounting Point 3		
Coordinate Direction	Predicted	Experimental
X_3	0.0110 (0.0280)	0.0120 (0.0305)
Y_3	0.0101 (0.0256)	0.0113 (0.0287)
Z_3	0.0072 (0.0183)	0.0109 (0.0277)

TABLE 2

PREDICTED MAXIMUM DISPLACEMENT MAGNITUDE FOR COMPRESSOR DURING SHUT-DOWN AND COMPARISON WITH AVAILABLE EXPERIMENTAL DATA

Spring Mounting Point 1		
Coordinate Direction	Predicted [in(cm)]	Experimental [in(cm)]
X_1	0.110 (0.279)	0.100 (0.254)
Y_1	0.182 (0.462)	n.a.
Z_1	0.101 (0.256)	0.040 (0.102)
Spring Mounting Point 2		
Coordinate Direction	Predicted [in(cm)]	Experimental [in(cm)]
X_2	0.232 (0.590)	0.120 (0.304)
Y_2	0.014 (0.036)	0.030 (0.076)
Z_2	0.032 (0.081)	0.090 (0.228)
Spring Mounting Point 3		
Coordinate Direction	Predicted [in(cm)]	Experimental [in(cm)]
X_3	0.117 (0.297)	0.110 (0.279)
Y_3	0.179 (0.454)	n.a.
Z_3	0.083 (0.211)	n.a.